ENHANCING THE FRACTURE TOUGHNESS OF ADHESIVELY BONDED JOINTS USING 3D PRINTED STRUCTURED INTERFACES

Lorenzo García-Guzmán, Luis Távara, José Reinoso, Jesús Justo and Federico París

Grupo de Elasticidad y Resistencia de Materiales, Universidad de Sevilla, ETSI.
Camino de los Descubrimientos s/n, Spain
Email: lgarcia22@us.es, ltavara@us.es, jreinoso@us.es, jjusto@us.es, fparis@us.es
Web Page: http://www.germus.es

Keywords: Structured interfaces; Interlaminar damage; Fracture toughness; ALM

Abstract

The recent appearance of Additive Layer Manufacturing (ALM or 3D printing) techniques for composites allows different kind of interfaces to be designed. To explore the applicability of such techniques, the present investigation focus on a well stablished test used to measure the interlaminar fracture toughness by means of double cantilever beam (DCB) specimens. The coupons included flat and trapezoidal patterned surfaces along the interface. Specimens were manufactured using ALM techniques for long-fibre composites. The trapezoidal patterns along the structured interface included different amplitude (A) and wavelength (λ) values for different kind of specimens. DCB experimental results showed a remarkable increase of the fracture toughness when the ratio A/λ increases in comparison with the flat interface specimens. A theoretical model is presented which is able to predict, in an approximate manner, the increase in toughness for the trapezoidal interfaces. A numerical model including the presence of cohesive elements along the interfaces is also presented. The numerical model proved that an increase of the ratio A/λ is directly related to an increase in the fracture mixed mode along the interface crack. This fact explains the increase of the fracture toughness on the experimental campaign. Finally, a very satisfcatory correlation in the experimental, theoretical and numerical results is obtained.

1. Introduction

Nowadays, composite structures are increasing their use in different industrial applications. The joining of composites parts plays a major role within this kind of structures. Particularly, the use of adhesively bonded joints is widespread. A key parameter that characterizes the quality of the joint is the fracture toughness. The aim of the present investigation is to improve the fracture toughness of an interface by modifying its geometry. Previous investigations showed that interfaces that can be found in nature are not flat, moreover they follow specific patterns improving the interface performance. Structured interfaces can be defined as those whose contact surfaces (between adherents) are not defined by flat profiles. In practical applications, interfacial geometries with structured patterns constitute efficient topologies for improving the mechanical behaviour of adhesive joints [1, 2].

Additionally, the development of novel ALM techniques, enabling printing fibre-reinforced composite materials, opens new possibilities for the design of 3D printed composite specimens. Specifically, the fused filament fabrication (FFM) processes allow fibre-reinforced plastics (FRP) deposition to be performed. Composite properties obtained using this technique are reported in [3].

A previous research of the authors [4], combines the advantages of ALM together with benefits of structured interfaces. There, interfaces with trapezoidal patterns were proved to be a potential solution to replace current structural conceptions with cheaper, lighter and wise-design 3D printing.

Thus, the aim of the present investigation can be divided in: (i) to present and compare the load versus displacement evolution curves and fracture resistance properties of composite ALM Double Cantilever Beam (DCB) specimens with structured trapezoidal patterns and those corresponding to flat interface coupons, (ii) to enhance and generalize the theoretical model developed in [4], and (iii) to develop some numerical analysis using cohesive zone elements of the tested coupons.

2. Experimental program: coupon definitions and tests results

The tested DCB coupons were manufactured using the 3D printer MarkOne®, see [3] for details about the machine. Two kind of coupons were printed: (a) flat and (b) structured. The geometric dimensions of flat coupons were: axial length L = 169 mm, width W = 20 mm, thickness $h = h_1 + h_{flat} = 4$ mm, see Figure 1(a). Structured interface instances were manufactured with the same overall dimensions, consequently the only difference between flat and patterned cases regarded to the configuration of the last layers, which conformed the actual interface profile. Each of the two halves of the produced DCB coupons consisted of 25 layers with 0.1 mm in thickness of glass-fibre reinforced composite (yellow lines), h_1, and 15 nylon layers (grey lines) with 0.1 mm in thickness ($h_{flat} = 1.5$ mm) for flat half specimen, 25 nylon layers ($h_{str} = 2.5$ mm) for half structured specimen with amplitude value A = 1mm and 20 nylon layers ($h_{str} = 2.0$ mm) for half structured specimen with amplitude value A = 0.75 mm. Note that 5 nylon layers with structured pattern were part of the bulk material, while the rest of nylon layers composed the interface region.

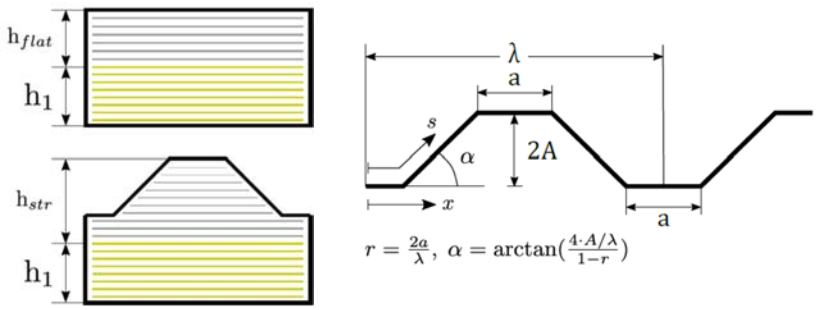

(a) (b)

Figure 1. (a) Zoom of the lateral view of the flat and structured coupons, including the printed layers. (b) Parameters defining the trapezoidal interface.

The material properties for each constituent corresponded to: $E_{11} = 25.84$ GPa, $E_{22} = 1.13$ GPa, $G_{12} = 0.88$ GPa and $\nu_{12} = 0.45$ for glass-fibre reinforced composite, E = 0.384 GPa and ν = 0.39 for nylon [3], and E = 4.231 GPa, G = 1.461 GPa for the adhesive layer [5]. Tested configurations were obtained combining λ = 4, 6, 8 mm, A = 0.75, 1 mm.

In order to see the influence of the structured patterns along the interface, two different critical energy release rate are defined:

- Effective critical energy release rate, G_c^x. This magnitude is associated to the energy dissipated during the crack propagation taking x-direction as reference, see Fig. 1(b), while the crack length is identified by a_x, and it is defined by:

$$G_c^x = -\frac{\partial \Pi_f(a_x)}{\partial (W.a_x)}; \quad (1)$$

where $\partial \Pi_f(a_x)$ is the energy dissipated during the crack propagation when the crack grows an area $\partial A_f = W\partial a_x$.

- Actual critical energy release rate, G_c^s. It is associated to the energy dissipated during the crack propagation taking s-direction as reference, see Fig. 1(b), which is identified with a curvilinear axis that follows the actual interface profile:

$$G_c^s = -\frac{\partial \Pi_f(a_s)}{\partial (W.a_s)}; \tag{2}$$

where $\partial \Pi_f(a_s)$ is the energy dissipated during the crack propagation when the crack grows an area $\partial A_f = W\partial a_s$.

Using [6], Π_f can be determined experimentally using the load-displacement curves obtained during the test. Thus, using (1) and (2), G_c^x and G_c^s, can be respectively obtained. Results obtained experimentally for the different analysed configuration are presented in Table 1. It should be noticed that geometrical configurations (iii), (vi) and (viii) were tested numerically, as will be presented in the following sections.

Table 1. G_c^x and G_c^s values obtained experimentally for several coupon configurations.

Specimen configuration	A (mm)	λ (mm)	G_c^x (J/m^2)	G_c^s (J/m^2)
Flat	-	-	136.3	136.3
(i)	0.85	8	274.0	236.8
(ii)	0.88	6	371.2	291.5
(iii)	0.85	4.75	-	-
(iv)	0.83	4	1231.2	760.9
(v)	0.63	6	262.1	228.2
(vi)	0.65	4.5	-	-
(vii)	0.70	4	484.0	345.4
(viii)	0.65	3.25	-	-

4. Simplified analytical model

In the present section a simplified analytical approach for G_c^x evaluation is presented, for further details see [7]. This approach is based on the formulation of a standard bilinear cohesive model, then the ratio between the energy release rate for shear loading, G_{II}, and the total energy release rate, G_T, can be defined by:

$$B = \frac{G_{II}}{G_T} = \frac{\frac{k_t}{k_n}\beta^2}{1-2\beta+(1+\frac{k_t}{k_n})\beta^2}, \quad \text{with} \quad \beta = \frac{\Delta_s}{\Delta_s+\Delta_n} = \frac{\sin\alpha}{\sin\alpha+\cos\alpha}, \tag{3}$$

where α is the angle of the sloped region of the joint section, Δ_n and Δ_s stand for the normal and tangential displacement of the adhesive, respectively, β identifies the mixed-mode ratio, G_{II} is the energy released in Mode II and $G_T = G_I + G_{II}$ is the total energy released, that is, the sum of energies in mode I and mode II. Thus, G_c^x is given by:

$$G_c^x = m_1^x G_{1c}^x + m_2^x[B^\eta G_{IIc} + (1-B^\eta)G_{Ic}], \quad \text{with } m_1^x = \frac{l_h}{\lambda},\ m_2^x = \frac{l_i}{\lambda}, \tag{4}$$

where l_i and l_h, correspond with the percentage in length for the inclined regions and for the horizontal regions, respectively.

5. Numerical analysis

The numerical analysis includes simulations using the FE package ABAQUS under the assumption of a large displacements response. The adhesive layer was modelled using CZM elements. Several configurations were modelled obtaining a very good agreement on the force-displacement response curve. In Figure 2, the experimental curves obtained for specimens with configuration (ii), according to Table 1, are compared with that numerically obtained.

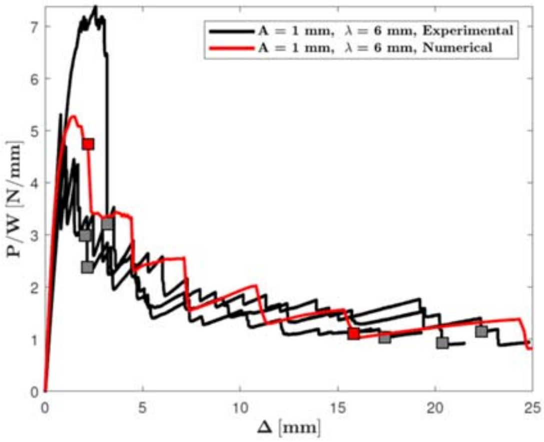

Figure 2. Numerical and experimental load-displacement curves for the specimen configuration (ii), A=0.88 mm and λ = 6 mm.

6. Comparison of the results obtained by experiments, analytical model and FEA

Table 2 summarises the obtained results using the different approaches presented in the present investigation. It is interesting to recall that the differences between the experimental and numerical data are in good agreement in most of the cases. Regarding the simplified theoretical approach, although it is able to capture qualitatively the effect of A and λ, it usually overestimates the fracture toughness values.

Table 2. Comparison of the G_c^x values obtained by experiments, analytical model and FEA.

Specimen configuration	Experimental G_c^x (J/m^2)	Analytical model G_c^x (J/m^2)	Numerical model G_c^x (J/m^2)
(i)	274.0	395.8	245.9
(ii)	371.2	706.9	402.0
(iii)	-	1001.0	713.8
(iv)	1231.2	1276.7	1004.6
(v)	262.1	387.8	265.0
(vi)	-	687.8	470.7
(vii)	484.0	963.7	676.5
(viii)	-	1203.4	963.8

7. Conclusions

In the present investigation, the fracture performance of 3D printed composite DCB coupons with structured patterns has been analysed. In particular, the interface profiles include trapezoidal patterns, which endowed a good compromise between fracture resistance capabilities and geometrical termination. The mechanical responses of such specimens have been analysed from experimental, theoretical and numerical points of view, with different aspect ratios A/λ (where A and λ are the amplitude and wavelength of the interface profile, respectively). These specimens exhibited a fracture resistance increase up to 900% with respect to standard flat interface profiles.

Acknowledgments

The work was supported by the Junta de Andalucía and European Social Fund (Project P12-TEP-1050), the Spanish Ministry of Economy and Competitiveness and European Regional Development Fund (Projects MAT2015-71036-P and MAT2015-71309-P).

References

[1] Srivastava, A., Osovski, S., Needleman, A. Engineering the crack path by controlling the microstructure. Journal of the Mechanics and Physics of Solids 2017;100:1-20.
[2] Maloney, K., Fleck, N. Damage tolerance of an architected adhesive joint. International Journal of Solids and Structures 2018; 132-133: 9-19.
[3] Justo J, Távara L, García-Guzmán L, París F. Characterization of 3D printed long fibre reinforced composites. Composite Structures 2018;185:537–48.
[4] García-Guzmán, L., Távara, L., Reinoso, J., Justo, J., París, F. Fracture resistance of 3d printed adhesively bonded dcb composite specimens using structured interfaces: Experimental and theoretical study. Composite Structures 2018;188:173-184.
[5] Guess, T., Reedy, E., Stavig, M. Mechanical properties of hysol ea-9394 structural adhesive. Tech. Rep.; Sandia National Laboratories; Albuquerque, New Mexico 87185 and Livermore, California 94550; 1995.
[6] Airbus. Carbon Fibre Reinforced Plastics. Determination of fracture toughness energy of bonded joints. Mode I. G1C. Issue 1. AITM 1-0053 2006.
[7] García-Guzmán, L., Reinoso, J., Távara, L., Justo, J., París, F. 3D printed trapezoidal interfaces for improved fracture response of adhesive joints in composite structures. Composite Science and Technology 2018 (submitted).